chemengineering

MDPI

Article

Kinetics of Simultaneous Ammonium and Phosphate Recovery by Natural Zeolite

Sandro Pesendorfer * and Markus Ellersdorfer

Chair of Process Technology and Industrial Environmental Protection, Montanuniversität Leoben, 8700 Leoben, Austria; markus.ellersdorfer@unileoben.ac.at

* Correspondence: sandro.pesendorfer@unileoben.ac.at

Abstract: Nowadays, fertilizers containing nitrogen and phosphorus are indispensable for medium and large-scale industrial agriculture. To meet the growing demand of nutrients and reduce the accompanied ecological footprint of primary fertilizer production, processes and technologies for nutrient recovery are necessary and have to be developed. This study represents the basis of an extension of the ion-exchange-loop-stripping process (ILS), which is a combined stripping and ion exchange process using natural zeolite for nitrogen recovery. In batch experiments with a special zeolite filled stirrer, the mechanism and kinetics of simultaneous ammonium and phosphate recovery by natural zeolite were determined. Zeolite loadings of 6.78 mg PO_4^{3-} g^{-1} were reached and after regeneration, phosphate recovery rates up to 75% of the initial concentration were achieved. The speed of phosphate precipitation is mostly controlled by the pH value of synthetic wastewater. Phosphate removal in simultaneous experiments does not affect ammonium sorption onto zeolite. These findings and the different removal mechanisms of ammonium and phosphate lead to versatile applications in wastewater treatment and reveal great potential of natural zeolite in simultaneous nutrient recovery processes.

Keywords: nutrient recovery; wastewater treatment; clinoptilolite

check for updates

Citation: Pesendorfer, S.; Ellersdorfer, M. Kinetics of Simultaneous Ammonium and Phosphate Recovery by Natural Zeolite. *ChemEngineering* **2021**, *5*, 68. https://doi.org/10.3390/chemengineering5040068

Academic Editor: Luis M. Gandía

Received: 14 September 2021
Accepted: 5 October 2021
Published: 8 October 2021

Publisher's Note: MDPI stays neutral with regard to jurisdictional claims in published maps and institutional affiliations.

Copyright: © 2021 by the authors. Licensee MDPI, Basel, Switzerland. This article is an open access article distributed under the terms and conditions of the Creative Commons Attribution (CC BY) license (https://creativecommons.org/licenses/by/4.0/).

1. Introduction

As a result of the constantly growing world population, the demand of organic and inorganic fertilizer for food production increases every year [1]. The major macronutrients nitrogen (N) and phosphorus (P) are produced in energy and resource intensive processes, e.g., the Haber-Bosch synthesis for nitrogen. On the other hand, overfertilization and the resulting eutrophication of surface and subsurface water present a global and persistent environmental problem [2,3]. Nutrient amounts in organic fertilizers like animal manure or biogas digestates are subject to fluctuations in process conditions, thus it is hard to fertilize plants with the appropriate quantity of nutrients. Additionally, harmful components in manure and sewage sludge, such as microplastics, germs, antibiotics and heavy metals accumulate in the soil and water. As a result of those problems the direct utilization of organic fertilizers in agriculture like manure, sewage sludge or biogas digestates is restricted by legal regulations of the European Commission [4]. Recycling is an essential element in modern industry, hence nutrient recycling by the selective recovery of N and P from organic wastewater could be the next step. Nutrient recovery can save energy in the primary production and prevent the contamination of soil and water by harmful substances. Industrial scaled processes use the precipitation of struvite to recover N and P from different wastewater streams [5–7]. Two disadvantages of these precipitation processes are the fixed N:P ratio in struvite and the possibility to separate recovered ammonium from phosphate. This study shows further development possibilities of the ILS process [8,9] and kinetics of a simultaneous recovery process of ammonium (NH_4^+) and phosphate (PO_4^{3-}) from aqueous solutions.

Ammonium recovery in the ILS process is based on the principle of ion exchange by zeolites especially clinoptilolites, which are micro- and mesoporous-aluminosilicate minerals. A unique property of natural clinoptilolite is the high selectivity for ammonium adsorption. Its low cost makes it one of the most commonly used zeolites to remove ammonium from wastewater [10–12]. The positively charged ammonium-ion is adsorbed onto the aluminosilicate crystal framework and in exchange the zeolite releases cations (e.g., Ca^{2+}, K^{+}, Na^{+} and Mg^{2+}) for charge balance in the aqueous solution. The adsorption capacity for ammonium on natural zeolite is in the range of 2.7–30.6 mg NH_4^{+} g^{-1} [12].

Few studies investigated the property to remove phosphate from wastewater due to electrostatic attraction, anion exchange or special pretreatment of the zeolite [13–17]. The mechanism of phosphate sorption onto the zeolite is determining the kinetics, capacity and removal rate of dissolved phosphate [18]. Simultaneous N- and P-removal based on phosphate precipitation were performed with synthetic zeolites from fly ash [19–21] and calcined dolomite [22]. Only Lin et al. [23] used natural zeolite with the main mineral clinoptilolite-Na for simultaneous N- and P-removal in a small scale laboratory setup. Zeolite has a very limited mechanical stability, which means in stirred batch processes there is no steady particle size distribution, in case zeolite can move freely. In contrast to others, this study shows batch experiments for simultaneous removal of phosphate and ammonium from synthetic wastewaters, in which the zeolite is fixed in a stirrer. The impacts of the pH value and initial concentration of N and P on the kinetics were also investigated. For zeolite regeneration and recovery, precipitated phosphate on the zeolite surface was dissolved in an acidic solution.

2. Materials and Methods

2.1. Materials

The zeolite was obtained from a Slovakian deposit and its main mineral is a calcium-bearing clinoptilolite. After crushing and sieving to 0.5–2.5 mm, zeolite was washed with distilled water to remove impurities and small particles formed by mechanical abrasion. Washed zeolite was dried at 105 °C for 24 h and stored in the desiccator. The BET specific surface area of the crushed and washed zeolite is 32.08 m^2 g^{-1} (nitrogen calibrated, Micromeritics Flowsorb 2300). A total of 30 g of zeolite were filled in a thin, rectangular shaped bag made from polypropylene (PP) net with the dimensions of 62 × 100 mm. The zeolite bag had a thickness of 4–5 mm and was stabilized between two PP frameworks (80 × 116 mm), which were held together by a PP cord. In brief, zeolite is fixed in a self-designed stirrer and immersed into synthetic wastewater. The thin layer ensured that the total amount of zeolite is in contact with the synthetic wastewater. Hence, the influence of a potential concentration gradient inside the layer of zeolite grains on the exchange kinetics can be neglected.

Experiments were carried out in a double jacket glass reactor with an inner diameter of 110 mm and a height of 220 mm. The reactor was tempered to 25 °C by a circulatory cooling unit (Julabo F250). During the experiments the reactor opening was covered with plates (PMMA) to prevent evaporation of the synthetic wastewater.

The synthetic wastewaters were a mixture of ammonium di-hydrogen phosphate ($(NH_4)H_2PO_4$) and ammonium chloride (NH_4Cl) dissolved in 2 L of distilled water. To increase the pH to 8 or 9, 1 M sodium hydroxide (NaOH) was added. All used chemicals were of analytical grade.

2.2. Simultaneous Exchange Experiments and P-Regeneration

At the beginning of each experiment, the stirrer was dipped into distilled water for 5 min to prevent distortion in the kinetics of the diffusion process due to capillary effects in pores. Exchange experiments were carried out for 24 h with a stirrer speed of 100 rpm. The double jacket glass reactor was filled with 1.5 L of synthetic wastewater, which was tempered to 25 °C. At time 0 min, the rotating zeolite stirrer was immersed into synthetic wastewater. After certain instants of time (30 or 60 min), a sample of 5 mL was taken

and filtered with a 0.45 µm syringe filter (Rotilabo-PVDF). The filtration ensured a clearly defined end of the exchange reaction, because small particles or free moving precipitates could affect the determination of N & P. Preliminary tests have shown that equilibrium is reached between 8 and 20 h. Hence, the samples after 21, 22, 23 and 24 h are defined to determine the equilibrium concentration, which was calculated as the arithmetic mean of these four values in each experiment.

To determine the kinetics of desorbed (exchanged) cations of the zeolite, an additional exchange experiment was performed with ammonium only.

After the simultaneous removal experiments, the ammonium and phosphate loaded zeolite stirrer was washed with distilled water and drained afterwards. For P-regeneration, the precipitated phosphate phases on the zeolite were dissolved in diluted sulfuric acid at pH 2.5. Compared to the exchange experiments, regeneration samples were taken in shorter periods because of faster reaction kinetics. Since the increasing pH slowed down the dissolution, another 2 mL of 1 M sulfuric acid was added after 3 h. P-regeneration ended after 4 to 5 h, when low P-loading (<1 mg PO_4^{3-} g^{-1}) of zeolite was achieved.

2.3. Analytical Methods and Calculations

Samples of the solution were diluted according to calibration lines. Afterward, the concentrations of N and P were determined photometrically by using Spectroquant® test kits for ammonium (Merck 1.14752.0001) and phosphate (Merck 1.4848.0002). A reference beam photometer (WTW photoLab 7600 UV-VIS) was used in the experiments. The initial concentrations of each synthetic wastewater were determined photometrically in triplicate. Temperature and pH value were measured with the pH meter inoLab pH7310. The desorbed cations (Ca^{2+}, K^+, Na^+, Mg^{2+}) were quantified by ICP-OES (ÖNORM EN ISO 11885:2009-11) at the Chair of Waste Processing Technology and Waste Management, Montanuniversiät Leoben.

The zeolite loading of ammonium and phosphate was calculated using the difference between initial and temporally decreasing concentration in solution related to the total mass of zeolite (see Equation (1)).

$$q_i = \frac{\left(c_{0,species} - c_{i,species}\right) * V_{solution}}{m_{zeo}} \quad (1)$$

q_i: zeolite loading at t = i (mg NH_4^+ g_{zeo}^{-1}, mg PO_4^{3-} g_{zeo}^{-1});
m_{zeo}: the amount of zeolite in the stirrer (g_{zeo});
$c_{0,species}$: the initial concentration of ammonium or phosphate (mg NH_4^+ L^{-1}, mg PO_4^{3-} L^{-1});
$c_{i,species}$: concentration at time t of ammonium or phosphate (mg NH_4^+ L^{-1}, mg PO_4^{3-} L^{-1});
$V_{solution}$: the volume of synthetic wastewater in reactor (L);
t: elapsed time (min).

2.4. Scanning Electron Microscope (SEM)

Samples of natural zeolite before and after N- and P-removal from synthetic wastewater were sputtered with carbon at the Chair of Resource Mineralogy, Montanuniversität Leoben, to ensure surface conductivity. The images of the zeolite surface were taken with a field emission gun (FEG) SEM LEO 1525 (Carl Zeiss AG, Oberkochen, Germany) at the Erich Schmid Institute of Materials Science (ESI).

3. Results

Table 1 gives an overview of the experimental runs (a–f) and their initial parameters which are compared in detail in the following Figures 1–5. Experiments (a_1) and (a_2) are ammonium exchange experiments with 259 and 514 mg NH_4^+ L^{-1}, which represent

basic experiments to determine and compare the single exchange performances with simultaneous removal experiments. All experiments were performed at least in duplicate.

3.1. Kinetics of Desorbed Cations

Figure 1 shows the cation kinetics, i.e., the amount of absorbed NH_4^+ during the single ammonium exchange experiment (a_1) in contrast to the type and the number of cations desorbed from the zeolite. Based on the cation kinetics, it is obvious that calcium is the dominant cation in the exchange reaction with untreated natural zeolite. After 4 h, zeolite absorbed 9.69 meq L^{-1} NH_4^+ and released 5.99 meq L^{-1} Ca^{2+}, 2.56 meq L^{-1} K^+, 0.61 meq L^{-1} Mg^{2+} and 0.39 meq L^{-1} Na^+ into the solution. As a result of ammonium sorption, pH increased from 5.47 to 6.39 during the experiment (24 h). The decreased ammonium concentration in the solution leads to a shifted NH_3/NH_4^+ equilibrium, which was readjusted by consuming hydronium ions (Equation (2)). The red solid line in Figure 1 shows the sum of the desorbed cations in meq L^{-1}. Compared to the line of absorbed ammonium (square indicators), it indicates the overall charge balance of the sorption process.

$$NH_4^+ \leftrightarrow NH_3 + H^+ \quad (2)$$

Table 1. Overview of initial parameters and zeolite loading at equilibrium and after 120 min.

		Initial Parameters			Zeolite Loading		
Figure	**Experiment**	**Ammonium**	**Phosphate**	**pH**	$q_{N,eq}$	$q_{P,eq}$	$q_P(120')$
		(g NH_4^+ L^{-1})	**(mg PO_4^{3-} L^{-1})**	**(-)**	**(mg NH_4^+ g^{-1})**	**(mg PO_4^{3-} g^{-1})**	**(mg PO_4^{3-} g^{-1})**
1	a_1	514	-	5.47	10.49	-	-
2	b	544	122	8.00	12.53	4.78	0.95
	c	257	126	8.02	8.32	3.84	0.77
3	c	257	126	8.02	8.32	3.84	0.77
	d	267	245	8.00	8.76	6.78	1.60
	a_2	259	-	8.03	8.30	-	-
4	c	257	126	8.02	8.32	3.84	0.77
	e	250	125	9.00	5.34	4.43	2.14
5	d	267	245	8.00	8.76	6.78	1.60
	f	263	246	9.00	6.01	4.09	2.67

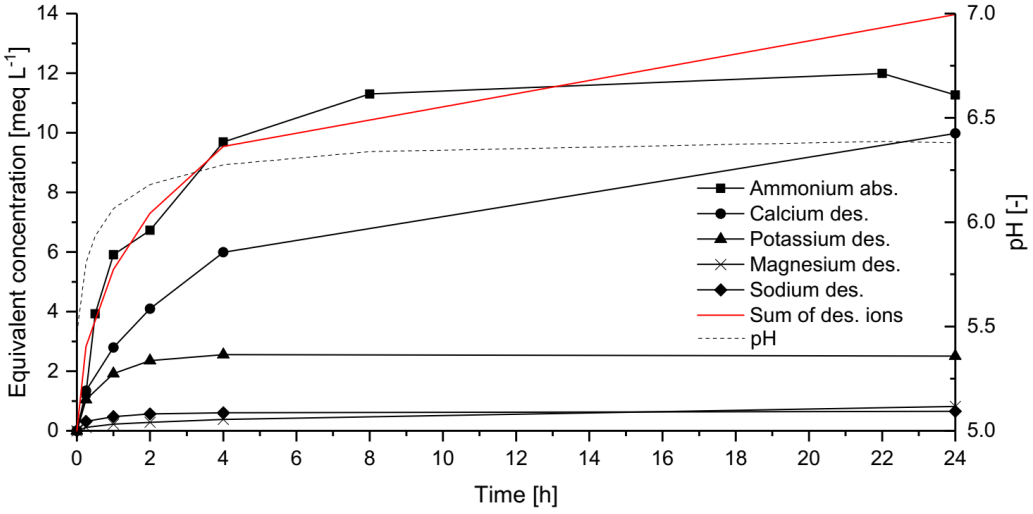

Figure 1. Equivalent concentrations of absorbed (NH_4^+) and desorbed (Ca^{2+}, K^+, Mg^{2+}, Na^+) cations over time. Line of absorbed ammonium is shown as the exchanged amount of equivalent concentration. Initial concentration: 514 mg NH_4^+ L^{-1}.

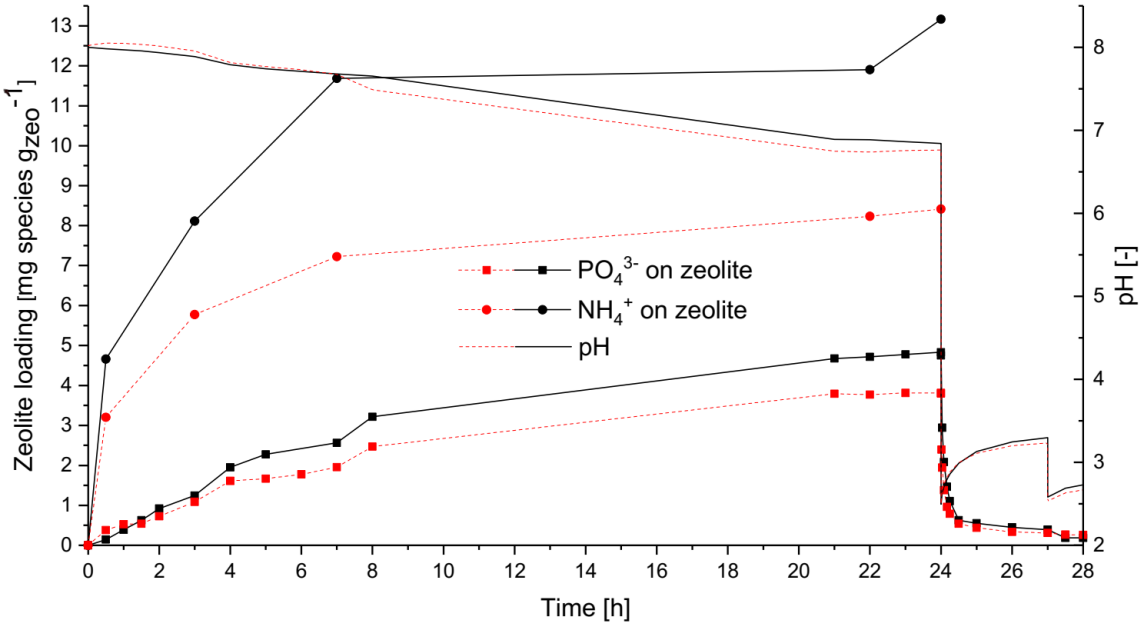

Figure 2. Effect of initial ammonium concentration at pH = 8 on P-removal. Initial values of experiments: black solid lines: 544 mg NH_4^+ L^{-1}, 122 mg PO_4^{3-} L^{-1}, pH = 8.00; red dashed lines: 257 mg NH_4^+ L^{-1}, 126 mg PO_4^{3-} L^{-1} pH = 8.02.

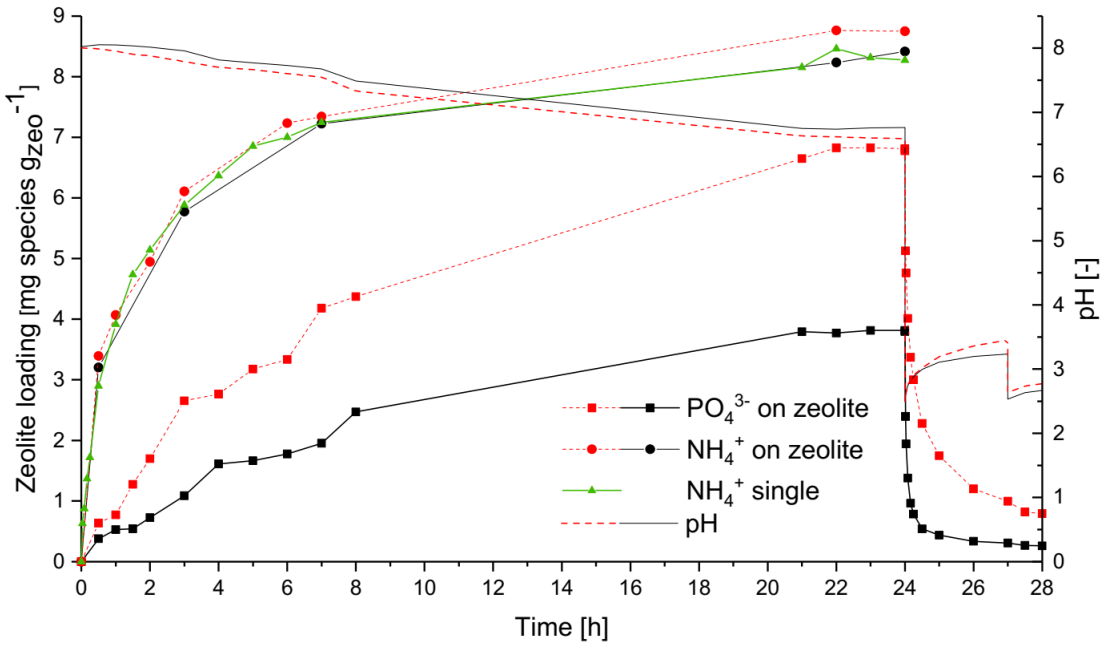

Figure 3. Effect of initial phosphate concentration at pH = 8 on P-removal. Initial values of experiments: black solid lines—257 mg NH_4^+ L^{-1}. 126 mg PO_4^{3-} L^{-1} pH = 8.02; red dashed lines: 267 mg NH_4^+ L^{-1}. 245 mg PO_4^{3-} L^{-1} pH = 8.00; green solid line: 259 mg NH_4^+ L^{-1} (ammonium only).

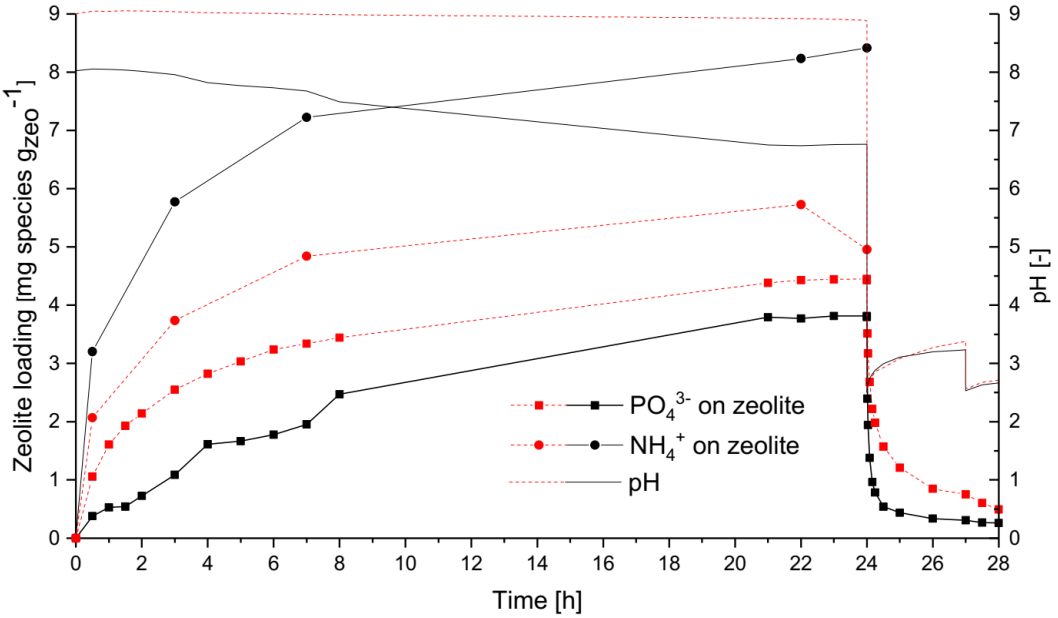

Figure 4. Effect of initial pH value on P-removal. Initial values of experiments: black solid lines: 257 mg NH_4^+ L^{-1}. 126 mg PO_4^{3-} L^{-1} pH = 8.02, removal rates: P = 61%, N = 65%; red dashed lines: 250 mg NH_4^+ L^{-1}. 125 mg PO_4^{3-} L^{-1} pH = 9.00, removal rates: P = 71% N = 43%.

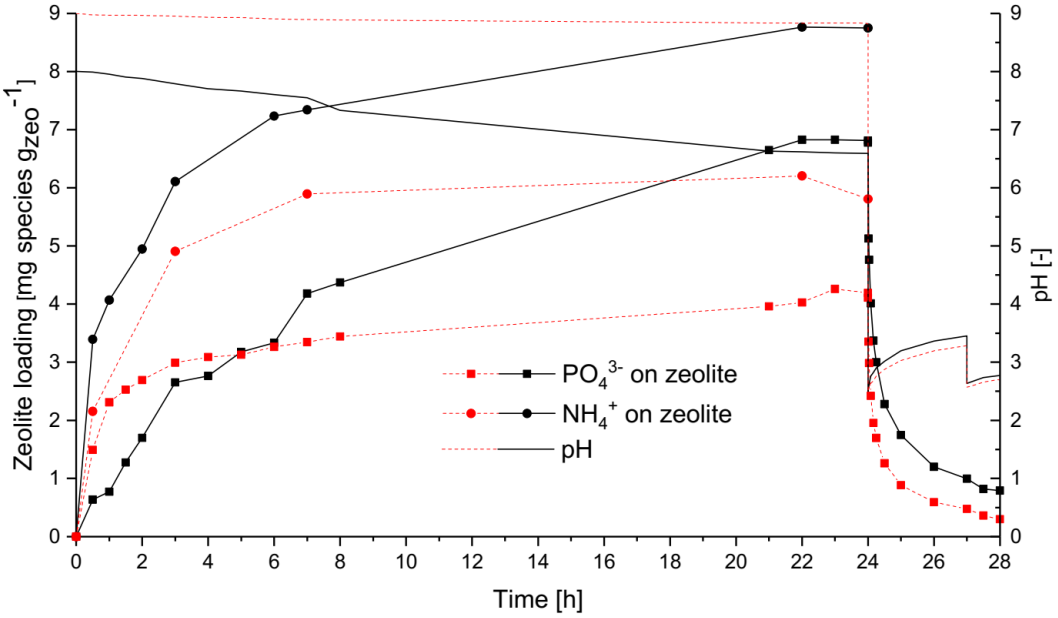

Figure 5. Effect of initial pH value at higher phosphate concentration. Initial values of experiments—black solid lines: 267 mg NH_4^+ L^{-1}. 245 mg PO_4^{3-} L^{-1} pH = 8.00, removal rates: P = 56%, N = 66%; red dashed lines: 263 mg NH_4^+ L^{-1}. 246 mg PO_4^{3-} L^{-1} pH = 9.00, removal rates: P = 34%, N = 46%.

3.2. Simultaneous Exchange Experiments (N & P)

In the following chapters, the results of simultaneous exchange experiments are described by comparing two experiments in each figure. Consequently, many of the occurred effects will be much easier to detect. Experiment (c) of Table 1 is defined as a standard experiment because, with these initial parameters, the first reproducible higher P-loadings on zeolite were achieved. The subsequent parameter study was based onto these initial parameters.

3.2.1. Effect of Initial Ammonium Concentration on N- and P-Removal

The first simultaneous exchange experiments show the impact of initial ammonium concentration on phosphate removal as indicated by experiments (b) and (c) (Figure 2). In contrast to the experiment (a_1), pH values decreased in both simultaneous experiments from 8 to 6.75 and 6.86, respectively. Experiment (b) starts with an ammonium concentration of 544 mg NH_4^+ L^{-1} and reached a zeolite N-loading at equilibrium of 12.53 mg NH_4^+ g^{-1} (circle indicators). Experiment (c) starts with 257 mg NH_4^+ L^{-1} and reached 8.32 mg NH_4^+ g^{-1} at equilibrium. Hence, higher initial N-concentration results in a higher N-loading but does not lead to more efficient N-removal (e.g., removal rate (b) 46% (c) 65%). At the beginning the sorption process, ammonium has a steep progression due to high concentration imbalance between zeolite and synthetic wastewater (high driving force for ion exchange). Over time, the exchange capacity of zeolite decreases, the sorption process becomes slower, and the curve flattens between 4 and 7 h.

In contrast, phosphate starts in both experiments at the same initial concentration (122 and 127 mg PO_4^{3-} L^{-1}) but different zeolite P-loadings (b: 4.78; c: 3.48 mg PO_4^{3-} g^{-1}) and P-removal rates (b: 80%; c: 61%) are reached at equilibrium (square indicators). The dissolution and recovery of the formed phosphate compound starts immediately after immersing the zeolite stirrer into diluted sulfuric acid (pH 2.5). After 4 h of P-recovery the zeolite loading stabilized at 0.18 and 0.26 mg PO_4^{3-} g^{-1}. At the end, the recovery solution comprises phosphate concentrations of 91 and 71 mg PO_4^{3-} L^{-1}, thus 75 and 57% of phosphate were recovered, respectively. Significant concentrations of Ca^{2+} were detected in the recovery solution, whereas K^+, Na^+ and Mg^{2+} were below detection limits.

3.2.2. Effect of Initial Phosphate Concentration at pH 8 on N- and P-Removal

Figure 3 shows the effect of the initial phosphate concentration on P-removal. Both experiments start with an ammonium concentration of (c) 257 mg NH_4^+ L^{-1} and (d) 267 mg NH_4^+ L^{-1} with a pH of 8. Ammonium sorption reveals similar progression and removal rates (c: 65%; d: 66%) in both experiments. For comparison, the green curve (triangle indicators) represents an exchange experiment (a_2) with ammonium only (initial concentration: 259 mg NH_4^+ L^{-1}). Therefore, a simultaneous P-removal has no effect on the ammonium exchange. Every ammonium loading line of a simultaneous experiment was approved with an additional ammonium experiment to check if a similar N-loading can be reached on zeolite.

Initial phosphate concentrations were 126 mg PO_4^{3-} L^{-1} and 245 mg PO_4^{3-} L^{-1}. Experiment (d) has a faster progression in P-removal and reaches higher equilibrium P-loading of 6.78 mg PO_4^{3-} g^{-1} compared to (c) 3.84 mg PO_4^{3-} g^{-1}. Consequently, higher initial phosphate concentrations lead to higher P-loadings on the zeolite at pH 8. Although the P-removal rate of (d) at 56% is slightly lower than (c) at 61%, substantially more phosphate was removed and recovered in (d).

Consequences of a higher P-loading are also seen in acid consumption during regeneration. The dissolution process of precipitated phosphate compounds in (d) is slower and pH value increases more than in (c), which indicates that more acid is needed to dissolve the higher amount of precipitated phosphate.

3.2.3. Effect of Initial pH Value on N- and P-Removal

Obviously, decreasing pH value is an indicator that hydronium ions participate or have an impact on the precipitation of phosphate. A higher pH value could affect the speed or equilibrium of the reaction positively. Figure 4 shows the standard experiment (c) compared to experiment (e), which has the same initial concentrations of N and P (250 mg NH_4^+ L^{-1}, 125 mg PO_4^{3-} L^{-1}) but starts at pH 9.

There are two clearly visible differences in the results of experiment (c) and (e), which show the impact of higher pH value on simultaneous removal. First, ammonium sorption at equilibrium is significantly lower at higher pH values (e) as the NH_3/NH_4^+ equilibrium is shifted to ammonia and less ammonium ions are available for the sorption process. Second,

the progression of phosphate removal is influenced by the pH value, compared to (c), the trend of P-removal in experiment (e) is much more like the N-removal curve, a reaction which starts at a higher speed and slows down when it strives for equilibrium. With 71%, the P-removal rate of (e) is higher compared to (c) with a value of 61%. Regeneration shows again slower dissolution and higher acid consumption in (e), which indicates a higher amount of precipitated phosphate on zeolite. In short, phosphate removal at pH 9 is much faster and more efficient than at pH 8. Contrastingly ammonium sorption is less efficient, due to shifted NH_3/NH_4^+ equilibrium.

3.2.4. Effect of Initial pH at Higher Phosphate Concentration on N- and P-Removal

Previous experiments showed that high initial phosphate concentration leads to elevated zeolite P-loadings in equilibrium (Section 3.2.2). Figure 5 shows the impact of pH on N- and P-removal at high initial phosphate concentration by comparing experiment (d) and (f). Experiment (d) reached the highest P-loading of all experiments at initial phosphate concentration of 245 mg PO_4^{3-} L^{-1} and pH 8. The same initial N and P concentrations were used in experiment (f) at pH 9. As determined in Section 3.2.3 higher pH leads to lower N-loading on the zeolite and overall lower N-removal, which were in (d) 66% and in (f) 46% in state of equilibrium. In the first 3 h P-removal at pH = 9 is faster and more efficient than P-removal at pH = 8. In an equilibrium state, P-loadings of zeolite are 6.78 mg PO_4^{3-} g^{-1} in (d) and 4.09 mg PO_4^{3-} g^{-1} in (f), which reveals the relative P-removal rates of 56% and 34%, respectively.

In summary, the following results were obtained from the laboratory experiments:

- Calcium is the preferred exchange ion in ammonium sorption;
- P removal is a precipitation reaction combined with ammonium sorption;
- High initial phosphate concentrations lead to high P-loadings;
- Speed of phosphate precipitation is controlled by pH;
- Ammonium sorption reduces at pH > 9.

3.2.5. Observations Regarding the Zeolite Surface

Two zeolite samples were analyzed by FEG-SEM. The surface of an unloaded natural zeolite is shown in Figure 6a. After simultaneous removal experiments, surface changed significantly. A fine textured crystal phase precipitated all over zeolite surface (Figure 6b). The second sample has a P-loading of 6.59 mg PO_4^{3-} g^{-1}, which is equal to the loading of experiment (d).

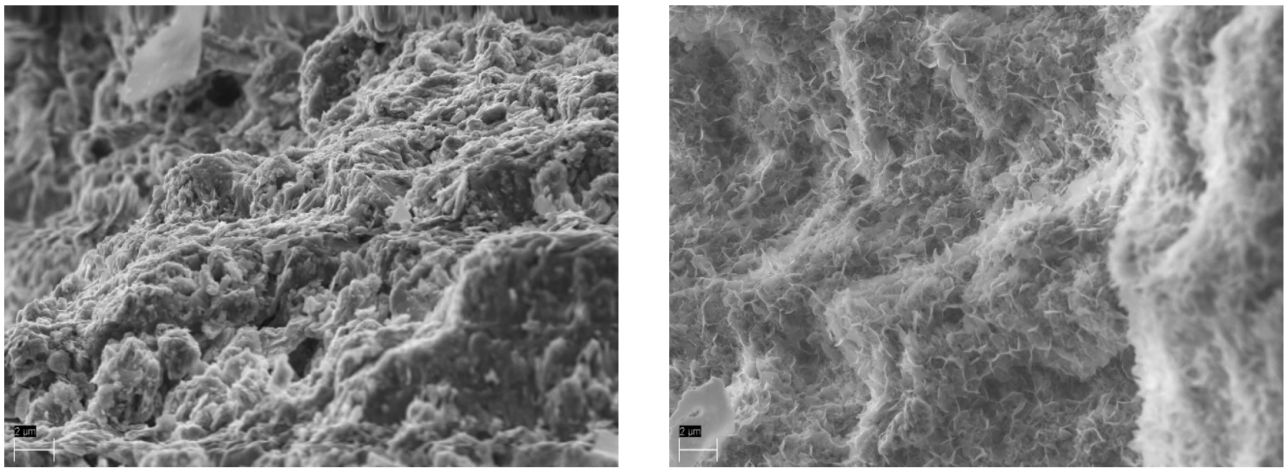

(**a**) (**b**)

Figure 6. FEG-SEM pictures of: (**a**) unloaded natural zeolite and (**b**) N & P loaded zeolite with precipitated CaP-phases.

4. Discussion

As shown in Figure 1, calcium is the preferred, desorbed cation in ammonium sorption and so, higher initial ammonium concentration leads to higher amounts of desorbed calcium ions. Analysis of the regeneration solution revealed that only calcium and phosphate were dissolved from the zeolite. Consequently, phosphate and calcium ions form a compound which is soluble in acid solutions. Significant concentrations of other ions such as NH_4^+, K^+, Mg^{2+} or Na^+ were not found in the regeneration solution, so the formation of magnesium ammonium phosphate (MAP) as a potential P-precipitate can be excluded. A doubled initial ammonium concentration results in a 19% higher P-removal rate at the same initial phosphate concentration. In short, higher initial ammonium concentration potentially leads to higher calcium desorption and further to higher P-removal (Figure 2), correlating to the findings of Lin et al. [23].

Higher initial phosphate concentration affects higher P-loading on zeolite (Figure 3), but the removal rate is lower than in experiment (c). Ammonium sorption reveals the same N-loadings in both experiments (c) and (d). Compared to the single ammonium experiment (a_2), simultaneous N and P removal has no impact on N-removal. An essential finding in Figure 3 is that P-loading is faster and higher in (d) with an equal calcium availability in case of equal initial ammonium concentrations. Hence, phosphate is the limiting factor in Figure 2, because a sufficient amount of calcium was desorbed due to higher ammonium sorption.

Increasing the initial pH value from 8 to 9 has a considerable effect on the rate of phosphate removal at the beginning of the experiment (Figure 4). Calcium phosphates (e.g., brushite and hydroxyapatite) are highly soluble in acid solutions, which could affect the slightly irregular progression at pH 8 compared to pH 9. Hermassi et al. [20] demonstrated that higher pH value encouraged the formation of hydroxyapatite and a lower pH the formation of brushite. Additionally, Macha et al. [24] detected a solubility minimum for differing calcium phosphates in the range of pH 8. In preliminary tests at pH < 7, it was not possible to precipitate phosphate on zeolite. All these findings lead to the possible chemical reaction (Equation (3)) formulated by Loehr et al. [25]

$$5Ca^{2+} + 4OH^- + 3HPO_4^- \leftrightarrow Ca_5OH(PO_4)_3 \downarrow + 3H_2O \quad (3)$$

This reaction is slow between pH 7 and 9. Higher pH values increase the precipitation of calcium phosphates (Figure S1), correlating to Lin et al. [23] A disadvantage of high pH value expresses in a lower ammonium sorption at pH 9, as a result of a shifted NH_3/NH_4^+ equilibrium. A further increase in the pH value led to a desorption of gaseous ammonia detected via ammonia warning device and accompanied by the typical strong smell. Unnoticed loss of gaseous ammonia would result in a falsely higher N-loading on zeolite, due to lower photometrically detected ammonium concentrations in the solution. Hence, pH 9 at 25 °C is the limit for ammonia removal with this laboratory setup to ensure no loss of ammonia.

In Figure 5 two significant parameters to reach a fast and high P-loading are combined (high pH and high initial phosphate concentration). Compared to experiment (e), phosphate precipitation in (f) is even faster at the beginning ($q_{P(120')}$ in Table 1: (e) 2.14 and (f) 2.67 mg PO_4^{3-} g^{-1}), due to high initial parameters. At equilibrium state P-loading of (f) is lower than (d) and even lower than (e), though initial phosphate concentration is doubled. Desorbed calcium reacts with dissolved phosphate near the zeolite surface and after simultaneous N- and P-removal, the whole surface is covered with precipitated calcium phosphates (Figure 6b). As a result of faster precipitation at pH 9, calcium phosphates probably form a denser layer on the zeolites surface and therefore reduce the area of ion exchange and affect low calcium desorption. The denser layer of calcium phosphate and low ammonium sorption at pH 9 lead to calcium limitations and finally to a low P-removal in experiment (f).

No abrasion of zeolite or precipitated calcium phosphates were detected in the reactor, which proves the functionality of the constructed stirrer to determine kinetics without affecting the particle size of zeolite. When the stirrer was washed with distilled water between N- and P-loading and P-regeneration, only small losses of phosphate (<0.70 mg PO_4^{3-} g^{-1}) occurred. This loss was detected as the difference between the amount of removed phosphate from the synthetic wastewater and the amount of recovered phosphate in regeneration solution. The successful P-removal and regeneration of each experiment was also confirmed by the remaining P-loadings on the zeolite, because solutions were completely exchanged between removal and regeneration and the majority of removed phosphate was found in regeneration solution.

After N- and P-loading, a white coating covered the inner bag (pp net) of the stirrer, which could not be removed by brushing or other mechanical stress. Dipping the inner bag into diluted sulfuric acid removed all of the white coating. Chemical analysis of sulfuric acid revealed that the white coating consists of calcium phosphate. The mechanical stability of these calcium phosphates underlines that hydraulic effects or higher flow rates in fixed bed columns do not remove precipitated phosphate from the zeolite surface.

5. Conclusions

In this study, natural zeolite was used to recover N and P from synthetic wastewater. The removal process shows great opportunity for a separate recovery of N and P. Experiments led to a better understanding of the P-removal mechanism and impacts of different parameters like pH value, ammonium sorption and initial phosphate concentration. A pH value between 8 and 9 reveals high and fast P-removal rates, which enables the application of a combined N- and P-removal in real wastewaters (e.g., sludge liquor, biogas digestates, pig manure), which are in the same range of pH. In the ILS process ammonium is recovered from the zeolite by sodium hydroxide using reversed ion exchange of ammonium sorption [26]. As precipitated calcium phosphate only dissolves in acid solutions, ammonium recovery in the ILS process with basic solutions has no impact on zeolites P-loading. On the other hand, separate phosphate recovery under acidic conditions is possible and would be a big advantage for nutrient recovery in order to enable many options for a further utilization of each nutrient.

Supplementary Materials: The following are available online at https://www.mdpi.com/article/10.3390/chemengineering5040068/s1, Figure S1: Ammonium and phosphate loading over time at pH 7/8/9.

Author Contributions: Conceptualization, S.P. and M.E.; methodology, S.P.; data curation, S.P.; writing—original draft preparation, S.P.; writing—review and editing, M.E.; visualization, S.P. All authors have read and agreed to the published version of the manuscript.

Funding: This research was funded by FFG—The Austrian Research Promotion Agency, grant number 864876 (ReNOx2.0).

Acknowledgments: The authors acknowledge the support during experiments in laboratory and helpful discussions at the office by Manuel Wassertheurer, Thomas Braunsperger and Stefan Niedermayer. Furthermore, thanks are also due to Kristina Stocker, Maik Zimmermann and Daniel Kiener for sample preparation and the visualization of the zeolite surface via FEG-SEM.

Conflicts of Interest: The authors declare no conflict of interest. The funders had no role in the design of the study; in the collection, analyses, or interpretation of data; in the writing of the manuscript, or in the decision to publish the results.

References

1. *World Fertilizer Trends and Outlook to 2022*; Food & Agriculture Organization of United Nations: Rome, Italy, 2019; ISBN 978-92-5-131894-2.
2. Withers, P.J.A.; Haygarth, P.M. Agriculture, phosphorus and eutrophication: A European perspective. *Soil Use Manag.* **2007**, *23*, 1–4. [CrossRef]

3. Carpenter, S.R.; Caraco, N.F.; Correll, D.L.; Howarth, R.W.; Sharpley, A.N.; Smith, V.H. Nonpoint Pollution of Surface Waters with Phosphorus and Nitrogen. *Ecol. Appl.* **1998**, *8*, 559–568. [CrossRef]
4. *Technical Proposals for the Safe use of Processed Manure above the Threshold Established for Nitrate Vulnerable Zones by the Nitrates Directive (91/676/EEC): EUR 30363 EN*; Publications Office of the European Union: Luxembourg, 2020.
5. Driessen, W.; Remy, M.; Hendrickx, T.; Haarhuis, R. Recovery of Phosphorus by Ormation of Struvite with the PHOSPAQ™ Process. European Biosolids and Organic Resources Conference. 2013. Available online: https://www.aquaenviro.co.uk/wp-content/uploads/2015/06/Driessen-W.-Pacques.pdf (accessed on 18 March 2020).
6. Lodder, R.; Meulenkamp, R. *Fosfaatterugwinning in Communale Afvalwaterzuiveringsinstallaties*; STOWA: Amersfoort, The Netherlands, 2011; ISBN 9789057735394.
7. Ueno, Y.; Fujii, M. *Phosphorus in Environmental Technologies: Full Scale Struvite Recovery in Japan*; IWA Pub: London, UK, 2004; ISBN 1843390019.
8. Ellersdorfer, M. The ion-exchanger-loop-stripping process: Ammonium recovery from sludge liquor using NaCl-treated clinoptilolite and simultaneous air stripping. *Water Sci. Technol.* **2018**, *77*, 695–705. [CrossRef] [PubMed]
9. Lubensky, J. *Verfahrensentwicklung des Ionentauscher-Loop-Strippings zur Gewinnung Eines Entstickungsmittels aus Abwässern—Vom Labormaßstab zur Pilotanlage. Dissertation*; Montanuniversität Leoben: Leoben, Austria, 2018.
10. Sherman, J.D. Ion Exchange Separations with Molecular Sieve Zeolites. In *Zeolites: Science and Technology*; Ribeiro, F.R., Rodrigues, A.E., Rollmann, L.D., Naccache, C., Eds.; Springer: Dordrecht, The Netherlands, 1984; pp. 583–623, ISBN 978-94-009-6130-2.
11. Kallo, D. Applications of Natural Zeolites in Water and Wastewater Treatment. *Rev. Mineral. Geochem.* **2001**, *45*, 519–550. [CrossRef]
12. Wang, S.; Peng, Y. Natural zeolites as effective adsorbents in water and wastewater treatment. *Chem. Eng. J.* **2010**, *156*, 11–24. [CrossRef]
13. Guaya, D.; Valderrama, C.; Farran, A.; Armijos, C.; Cortina, J.L. Simultaneous phosphate and ammonium removal from aqueous solution by a hydrated aluminum oxide modified natural zeolite. *Chem. Eng. J.* **2015**, *271*, 204–213. [CrossRef]
14. Mitrogiannis, D.; Psychoyou, M.; Baziotis, I.; Inglezakis, V.J.; Koukouzas, N.; Tsoukalas, N.; Palles, D.; Kamitsos, E.; Oikonomou, G.; Markou, G. Removal of phosphate from aqueous solutions by adsorption onto Ca(OH) 2 treated natural clinoptilolite. *Chem. Eng. J.* **2017**, *320*, 510–522. [CrossRef]
15. Mitrogiannis, D.; Psychoyou, M.; Koukouzas, N.; Tsoukalas, N.; Palles, D.; Kamitsos, E.; Pantazidis, A.; Oikonomou, G.; Baziotis, I. Phosphate recovery from real fresh urine by $Ca(OH)_2$ treated natural zeolite. *Chem. Eng. J.* **2018**, *347*, 618–630. [CrossRef]
16. Jiang, C.; Jia, L.; He, Y.; Zhang, B.; Kirumba, G.; Xie, J. Adsorptive removal of phosphorus from aqueous solution using sponge iron and zeolite. *J. Colloid Interface Sci.* **2013**, *402*, 246–252. [CrossRef] [PubMed]
17. Guaya, D.; Valderrama, C.; Farran, A.; Cortina, J.L. Modification of a natural zeolite with Fe(III) for simultaneous phosphate and ammonium removal from aqueous solutions. *J. Chem. Technol. Biotechnol.* **2016**, *91*, 1737–1746. [CrossRef]
18. Loganathan, P.; Vigneswaran, S.; Kandasamy, J.; Bolan, N.S. Removal and Recovery of Phosphate from Water Using Sorption. *Crit. Rev. Environ. Sci. Technol.* **2014**, *44*, 847–907. [CrossRef]
19. You, X.; Valderrama, C.; Cortina, J.L. Simultaneous recovery of ammonium and phosphate from simulated treated wastewater effluents by activated calcium and magnesium zeolites. *J. Chem. Technol. Biotechnol.* **2017**, *92*, 2400–2409. [CrossRef]
20. Hermassi, M.; Valderrama, C.; Gibert, O.; Moreno, N.; Font, O.; Querol, X.; Batis, N.H.; Cortina, J.L. Integration of Powdered Ca-Activated Zeolites in a Hybrid Sorption–Membrane Ultrafiltration Process for Phosphate Recovery. *Ind. Eng. Chem. Res.* **2016**, *55*, 6204–6212. [CrossRef]
21. Hermassi, M.; Dosta, J.; Valderrama, C.; Licon, E.; Moreno, N.; Querol, X.; Batis, N.H.; Cortina, J.L. Simultaneous ammonium and phosphate recovery and stabilization from urban sewage sludge anaerobic digestates using reactive sorbents. *Sci. Total Environ.* **2018**, *630*, 781–789. [CrossRef] [PubMed]
22. Pesonen, J.; Myllymäki, P.; Tuomikoski, S.; Vervecken, G.; Hu, T.; Prokkola, H.; Tynjälä, P.; Lassi, U. Use of Calcined Dolomite as Chemical Precipitant in the Simultaneous Removal of Ammonium and Phosphate from Synthetic Wastewater and from Agricultural Sludge. *ChemEngineering* **2019**, *3*, 40. [CrossRef]
23. Lin, L.; Wan, C.; Lee, D.-J.; Lei, Z.; Liu, X. Ammonium assists orthophosphate removal from high-strength wastewaters by natural zeolite. *Sep. Purif. Technol.* **2014**, *133*, 351–356. [CrossRef]
24. Macha, I.; Boonyang, U.; Cazalbou, S.; Ben-Nissan, B.; Charvillat, C.; Oktar, F.; Grossin, D. Comparative study of Coral Conversion, Part 2: Microstructural evolution of calcium phosphate. *J. Aust. Ceram. Soc.* **2015**, *51*, 149–159.
25. Loehr, R.C.; Prakasam, T.B.S.; Srinath, E.G.; Yoo, Y.D. *Development and Demonstration of Nutrient Removal from Animal Wastes*; EPA Report R2-73-095; U.S. Government Printing Office: Washington, DC, USA, 1973.
26. Lubensky, J.; Ellersdorfer, M.; Stocker, K. Ammonium recovery from model solutions and sludge liquor with a combined ion exchange and air stripping process. *J. Water Process Eng.* **2019**, *32*, 100909. [CrossRef]